PCCP

Degradation reaction of monoethanolamine using TS-1 zeolite as a photocatalyst

Takayuki Ban, Satoshi Kondoh, Yutaka Ohya and Yasutaka Takahashi

Department of Chemistry, Gifu University, 1-1 Yanagido, Gifu 501-1193, Japan

Received 13th August 1999, Accepted 26th October 1999

Photocatalytic properties of TS-1 zeolite were examined *via* a degradation reaction of monoethanolamine (MEA). When TS-1 was mixed with MEA aqueous solution, the MEA molecules were bonded to the Ti atoms in TS-1 since the latter were coordinatively unsaturated. In fact, the Ti atoms in TS-1 were isolated and coordinated by four oxygen atoms. The change in the coordinative situation around the Ti atom shifted the absorption of ultraviolet (UV) light from about 220 nm, which is intrinsic absorption of TS-1, to a longer wavelength, *i.e.* around 300 nm. When the suspension mixture of TS-1 and MEA aqueous solution was irradiated by UV light with a wavelength of around 300 nm, photo-excitation of the MEA-adsorbed Ti species took place leading to a degradation of MEA molecules. Although a photocatalytic activity per weight of a specimen was lower for TS-1 than for TiO_2, the activity per Ti atom in TS-1 was higher than that in TiO_2. The strong adsorption of MEA to TS-1 and its microporous structure are attributed to the high activity of the photocatalytic reaction. The use of either TS-1 or TiO_2 as a photocatalyst had no effect on the kind of products and the product ratios.

1 Introduction

Zeolites are crystalline tectoaluminosilicates that have cavities or channels smaller in size than 2 nm, which are able to recognize, discriminate, and organize molecules with slight differences within 0.1 nm. The zeolites are widely used in many chemical and physical processes such as catalysis reactions, ion exchanges, separations, and chemical sensing technologies.[1–5] If the zeolites are applied to a photocatalyst, it would be possible to realize the unique photocatalyst with a molecular selectivity. However, a modification of the framework and/or within the channels of zeolites is necessary because aluminosilicate zeolites are transparent in a wavelength range of UV-Vis light. Since a synthesis of TS-1 zeolite by Taramasso *et al.*,[6] who modified the framework of silicalite-1 (SiO_2) *via* an isomorphic substitution of Si in it for Ti, many kinds of metallosilicate zeolites containing metal atoms such as Ti, V, Mn, Zn and Fe in the framework have been synthesized and investigated.[7–23] Although TS-1 zeolite absorbs only UV light with very short wavelength around 220 nm, Anpo and coworkers showed that a decomposition reaction of NO[24] and a reduction of CO_2 with H_2O[25–27] were photocatalyzed in the presence of TS-1. In the decomposition of NO, TS-1 led to the formation of N_2 and O_2 and showed a high activity, while TiO_2 resulted in the formation of N_2O and O_2.[24] In the reaction of CO_2 and H_2O, the use of TS-1 led to the formation of methane and methanol, while TiO_2 yielded only methane.[25–27] Afterwards, some workers have studied the photocatalytic reaction using titanosilicate zeolites or mesoporous materials with larger channels in order to increase the reaction rate.[28–32] However, an application of metallosilicate zeolite to a photocatalytic treatment of wastewater has not been examined at all. So far, some workers investigated the influence of water or NH_3 aqueous solution on the framework structure of titanosilicate zeolite.[33–41] Their investigations *via* XPS,[33] IR,[34,35] Raman,[34] UV-Vis,[34–37] and XANES measurements[38–41] suggested that water or NH_3 molecules were adsorbed to 4-fold coordinated Ti atoms in zeolite to give 6-fold coordinated ones. If a photoexcitation of the Ti sites modified by organic molecules can lead to a degradation of the organic compounds, an interesting photocatalytic reaction can be expected, and TS-1 can be applied as a photocatalyst with a molecular selectivity.

Semiconductor photocatalysts such as TiO_2 have been extensively investigated and used for the treatment of wastewater. In the photocatalytic reaction using TiO_2, electron and hole in conduction and valence bands formed *via* photoexcitation of TiO_2 contribute to the reduction and oxidation reactions, respectively, as shown in Fig. 1(b). On the other hand, in a photocatalytic reaction using TS-1, charge transfer excitation in the Ti species modified *via* the adsorption of organic compounds, that is, Ti^{4+}-$O^{2-} \rightarrow Ti^{3+}$-$O^{-}$, is expected to lead to photocatalytic reactions, as shown in Fig. 1(a). Depending on whether TS-1 or TiO_2 is used as a photocatalyst, different

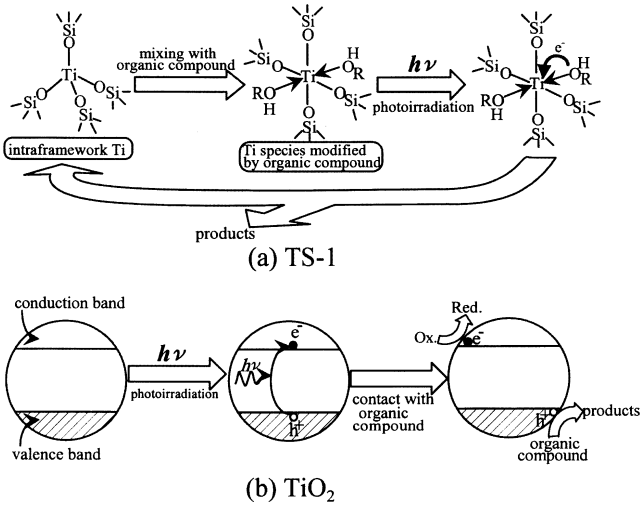

Fig. 1 Anticipated photocatalytic reactions using (a) TS-1 and (b) TiO_2.

reaction products may result because a different reaction process is involved. Other unique photocatalytic properties are also anticipated.

In this study, we examined how the adsorption of organic compounds such as alkanolamine on Ti atom in TS-1 influenced the UV-Vis spectra. It was also examined whether the adsorbed alkanolamine molecules are photocatalytically decomposed as shown in Fig. 1.

2 Experimental procedures

2.1 Preparation of TS-1

TS-1 zeolite was synthesized from an aqueous solution containing tetraethyl orthosilicate ($Si(OEt)_4$), triethanolaminatotitanium *i*-propoxide ($Ti((OC_2H_4)_3N)(OPr^i)$) and tetra-*n*-propylammonium hydroxide (NPr^n_4OH) as a template agent *via* a hydrothermal treatment. At first, 50.00 g of 10 wt.% NPr^n_4OH aqueous solution, which contained 25.0 mmol of NPr^n_4OH, was cooled in an ice bath. Then, 12.75 g (61.25 mmol) of $Si(OEt)_4$ was added into the solution under stirring, followed by stirring for 1 h at 0 °C. In the next step, 0.20 ml of 80 wt.% $Ti((OC_2H_4)_3N)(OPr^i)$ propan-2-ol solution, which contained 1.25 mmol of $Ti((OC_2H_4)_3N)(OPr^i)$, was added dropwise into the solution, followed by stirring for 4 h at 0 °C. The chemical composition of the solution was adjusted to $TiO_2 : SiO_2 : NPr^n_4OH : H_2O = 0.01 : 0.49 : 0.20 : 20$, that is, $Ti/(Si + Ti) = 0.02$. The solution was transferred into a teflon-lined autoclave and then heat-treated at 170 °C under an autogenous pressure for 1 week. A prepared powder was separated by centrifugation, washed using 1000 ml of distilled water and then heat-treated at 600 °C for 15 h in a flow of air in order to remove the template agent. Thus prepared powder was used as a TS-1 specimen. A silicalite-1 specimen was prepared *via* the same procedure without the Ti source.

2.2 Characterization of the specimens

Crystalline phases in the prepared specimens were examined *via* powder X-ray diffraction (XRD) measurements (Rigaku Geigerflex RAD-2R) using Cu-Kα radiation monochromated by graphite. The measurements were conducted with a scan speed of 2° min^{-1} for a scanning range between 10 and 70° in terms of 2θ. Lattice constants were estimated *via* Rietveld analysis of XRD pattern recorded for a mixture of the specimen and crystalline Si powder for a reference. The XRD pattern for the estimation of lattice constants was measured in a step scan mode with a step width of 0.02° and a fixed time of 10 s for a scanning range between 20 and 80° in 2θ. The Rietveld analysis was conducted using software of RIETAN 94 written by Izumi.[42]

Thermal analysis (TG-DTA measurements, Shimadzu, Model DT-40) was conducted in order to examine the combustion temperature of the template agent using 20 mg of the specimen before the heat treatment at 600 °C. TG-DTA curves were recorded in a flow of air in a temperature range between 25 and 1000 °C at a heating rate of 5 °C min^{-1}.

Diffuse reflectance ultraviolet-visible (DR-UV-Vis) spectra (Hitachi, Model U4000) were measured in a wavelength range between 200 and 1500 nm using a $BaSO_4$-lined integration sphere (ϕ 60 mm). An α-Al_2O_3 disk was used as a reference. For powder specimens, a pellet (ϕ 10 mm) was made from 0.3 g of the specimen at an uniaxial press of 0.1 t cm^{-2} under a reduced pressure of 0.05 mmHg, and set to a sample holder with a hole (ϕ 8 mm). For suspension specimens, the specimen was put into a quartz glass cell (3 × 10 × 45 mm, Nippon Quartz Glass Co.) for the measurement. All spectra were reduced according to Kubelka–Munk theory;[43] $F(R) = (1 - R)^2/2R$, where $F(R)$ is the Kubelka–Munk function and R is reflectance. When the Kubelka–Munk function is less than 3, a peak area is proportional to a concentration of an absorbant.[43]

UV-Vis spectra (Hitachi, Model U3500) of liquid specimens were collected in a transmittance mode using a dual beam. The specimens were put into a quartz glass cell (10 × 10 × 45 mm, Nippon Quartz Glass Co.). An empty cell was used as a reference.

Infrared (IR) spectra (Perkin Elmer, Model 2000 FT IR) of solid specimens were measured in a wavenumber range between 450 and 4500 cm^{-1} *via* a KBr method. A very small amount of the specimen was mixed with 0.15 g of KBr powder. It was uniaxially pressed at 0.05 t cm^{-2} under a reduced pressure of 0.05 mmHg to give a translucent pellet.

The specific surface area (Japan Bel Co., Model BELSORP 28SA) was measured *via* a BET method using N_2-gas adsorption. The specimens were pre-treated at 200 °C under 0.05 mmHg for 2 h. An adsorption isotherm was measured at 77 K in a relative pressure range from 0.15 to 0.40.

2.3 Photocatalytic reactions

A reactant solution with a concentration of MEA of 0.5 mM was prepared from milli-Q water and MEA. The pH value of the solution was 9.8. The powder of TS-1 was added into the solution and an added amount of TS-1 was adjusted to 0.5 g L^{-1}. The suspension was stirred for 40 min in the dark and then transferred into a test tube (ϕ 10 mm) made of quartz glass. A photoirradiation was conducted under stirring using a light from super high pressure Hg lamp, which was passed through an optical filter (Toshiba Glass Co., UV-D33S) and water in order to cut UV light with short wavelength and infrared radiation, respectively. The UV-Vis spectrum of the optical filter itself showed a maximum transmittance of 89% at 324 nm and transmittance larger than 50% in the wavelength range between 252 and 393 nm. As references, silicalite-1, which has the same crystal structure as TS-1 and a chemical composition of SiO_2, and TiO_2 (Degussa P-25), which consists of anatase and very small amount of rutile, were used.

The photocatalytic decomposition of MEA was also examined *via* photoirradiation while bubbling N_2 or O_2 gas. The bubbling of N_2 and O_2 was conducted in order to eliminate and increase soluble O_2, respectively. These gases were bubbled into 6 ml of the suspension containing 0.5 g L^{-1} of the specimen powder from its bottom using a needle with an inside diameter of 0.5 mm at a flow rate of 2 L min^{-1}. The bubbling of the gas was carried out for 60 min before the photoirradiation and continued also during the photoirradiation. The photoirradiation was conducted under stirring using a light from super high pressure Hg lamp, which was passed through the above-mentioned optical filter and water.

The photoirradiated suspensions were filtered using a membrane with a pore size of 0.20 μm. The components in the solutions were characterized *via* high performance liquid chromatography (HPLC). The amine components such as monoethanolamine, glycine (H_2NCH_2COOH), and ammonia were detected using a separation column for cation analysis (Tosoh Co., IC-CATION SW model) *via* a change of conductivity (Tosoh Co., Model IC-8010). A 2.5 mM of HNO_3 solution with H_2O and acetonitrile (CH_3CN) as solvents, in which $H_2O : CH_3CN = 1$ v/v, was used as a mobile phase. The flow rate was 0.6 mL min^{-1}. The components of some aldehydes and carboxylic acids were detected using a separation column for anion analysis (Tosoh Co., Model OA PAK-A) *via* changes of conductivity (Tosoh Co., Model CM-8020) and absorbance of UV light at 210 nm (TOSOH Co., Model PD-8020). A 0.75 mM of H_2SO_4 aqueous solution was used as a mobile phase. The flow rate was 0.8 mL min^{-1}.

3 Results and discussion

3.1 Characterization of a prepared specimen

Just after the hydrothermal synthesis the powder was characterized *via* TG-DTA measurement. The thermograms showed

an exothermic peak with a large weight loss around 400 °C. This may be assigned to the combustion of the template agent, NPr^n_4OH. An amount of the template agent in the specimen was estimated at $Si_{96-x}Ti_xO_{192}\cdot 4NPr_4OH$ from the weight loss around 400 °C, which was consistent with the previous report.[44] No other endothermic or exothermic peaks and weight losses were observed. Because the template was burned off around 400 °C all at once, it can not be considered that the specimen, which was heat-treated at 600 °C, contained organic substances. The prepared specimen was characterized *via* XRD, DR-UV-Vis, and IR measurements. All the peaks observed in the peaks XRD patterns were assigned to MFI-type zeolite, into which TS-1 and silicalite-1 are classified. Because no peaks assignable to TiO_2 such as rutile and anatase were observed, the Ti atoms may be homogeneously incorporated into the zeolite.

Fig. 2(A) and (E) show DR-UV-Vis spectra of the TS-1 and silicalite-1 specimens, respectively. These figures clearly show that silicalite-1 had no absorption in the measured wavelength range, while TS-1 exhibited a peak at 220 nm assignable to an isolated and 4-fold coordinated Ti, indicating that all Ti atoms in the specimen were incorporated in the framework of the zeolite.[33,36,45–51] When the spectrum of the TS-1 specimen was examined in detail, absorption started at 300 nm and gradually became stronger with decreasing the wavelength of the irradiated light. This indicates that a small amount of 5-fold coordinated Ti species is present in the TS-1 specimen. The 5-fold coordinated Ti species may not be extra-framework Ti species and may form *via* a partial hydration of intra-framework Ti species by water in air.

It has been well known that the IR spectrum of zeolites with intra-framework Ti exhibits an absorption band around 960 cm^{-1}, which is absent for pure silica zeolites and characteristic of metal-substituted zeolites.[46,52–54] The peak may be assigned to a stretch mode of SiO_4 unit perturbed by neighbor Ti.[46,52–54] As clearly shown in Fig. 3, the TS-1 specimen exhibited an absorption around 960 cm^{-1}, while that of silicalite-1 specimen did not, confirming the presence of intra-framework Ti atoms in the TS-1. However, the peak was shifted to 970 cm^{-1}. This indicates that a small amount of 5-fold coordinated intra-framework Ti species formed in the TS-1 specimen *via* a partial hydration by water in air. The intensity ratio of the absorption peak at 960 cm^{-1} to that observed at 800 cm^{-1} in the IR spectrum can be used for the estimation of the chemical composition of the TS-1 specimen. The peak observed at 800 cm^{-1} remained regardless of the presence of intra-framework Ti, which may be assigned to a Si–O symmetric stretching vibration of SiO_4 units in the framework. The peak intensity ratio, $I(970\ cm^{-1}) : I(800\ cm^{-1})$, was found to be 0.45 for the TS-1 specimen. Using the

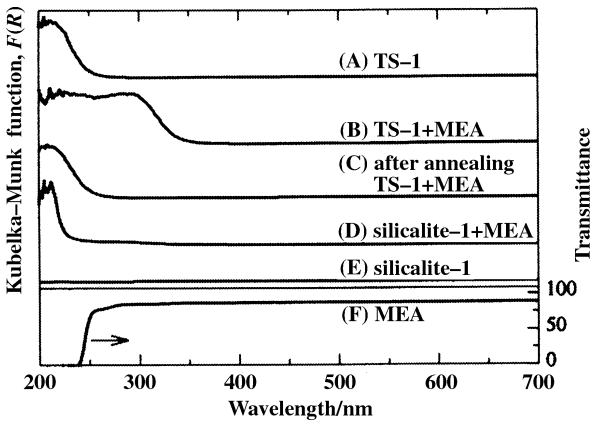

Fig. 2 UV-Vis spectra of (A) TS-1, (E) silicalite-1, (F) MEA, their mixtures; (B) TS-1 + MEA, and (D) silicalite-1 + MEA and (C) the specimen after annealing TS-1 + MEA at 600 °C.

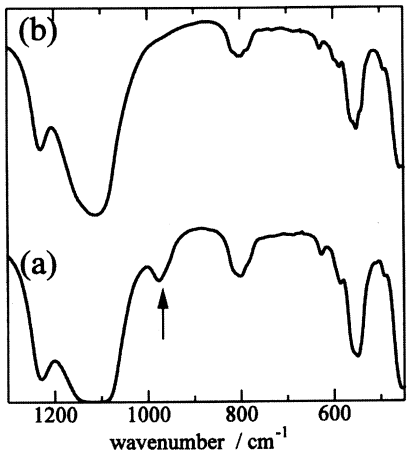

Fig. 3 IR spectra of (A) TS-1 and (B) silicalite-1. The arrow shows absorption around 960 cm^{-1}.

relation between $I(960\ cm^{-1}) : I(800\ cm^{-1})$ and the chemical composition reported by Tarramasso *et al.*[6] and Tuel,[55] the chemical composition of the TS-1 specimen was estimated at $Ti : (Ti + Si) = 0.013$ to 0.014. The lattice constants of TS-1 were estimated *via* Rietveld analysis of its XRD pattern: $a = 2.0097(1)$ nm, $b = 1.9925(1)$ nm and $c = 1.3403(1)$ nm, and the lattice volume was 5.367(1) nm^3, where the numbers in parentheses show a standard deviation. The chemical composition can also be estimated from the unit cell volume. Based on the relationship between the lattice volume and the chemical composition that was reported by Tarramasso *et al.*[6] and Tuel,[55] it was found that the TS-1 specimen has the chemical composition of $Ti : (Ti + Si) = 0.013$, that is, $Si_{0.987}Ti_{0.013}O_2$. The combined results of XRD and FTIR measurements clearly indicate that the chemical composition of the TS-1 specimen is supposed to be $Ti : (Ti + Si) = ca.$ 0.013, that is, $Si_{0.987}Ti_{0.013}O_2$, although a small amount of H_2O may also be present. Ti concentration in the prepared TS-1 specimen was lower than that in the starting solution. Our preliminary study indicated that when $Ti((OC_2H_4)_3N)(OPr^i)$ was used as a Ti source, excess Ti was removed during the washing process *via* a complex formation between Ti species and $N(C_2H_4OH)_3$.

3.2 Adsorption of various compounds to the Ti atoms in TS-1

In order to apply TS-1 as a photocatalyst, an organic compound that is appropriate for a photocatalytic reaction has to be selected. As the photocatalytic reaction was carried out using diluted aqueous solution of an organic compound, it is necessary for the organic compound to adsorb onto Ti site in TS-1 more preferentially than H_2O molecules and the used organic compound has to be small enough in size in order to enter and diffuse into the channel of TS-1 zeolite. The TS-1 specimen was mixed with various neat organic compounds such as alcohols and alkanolamines and their DR-UV-Vis spectra were measured. DR-UV-Vis spectra of the obtained suspensions are shown in Fig. 4, together with that of the TS-1 specimen itself. Although the spectra of the suspensions were measured just after the mixing and after aging for 1, 2 and 4 h, the peak intensities and profiles did not change with the aging time. All spectra of the suspensions showed peaks not only around 220 nm but also around 300 nm. Intensities of the absorption peak around 300 nm increased in the following order: $MeOH \leqslant N(C_2H_4OH)_3$ (TEA) < $EtOH \leqslant Pr^iOH < Bu^tOH < NH_3$ aq. < H_2O < MEA < $NH(C_2H_4OH)_2$ (DEA). The spectra of the suspensions containing alkanolamines such as MEA and DEA tended to exhibit more intense peaks around 300 nm than those containing alcohols, H_2O, and aqueous ammonia solution, and among the alcohol suspensions the alcohols with bulkier alkyl

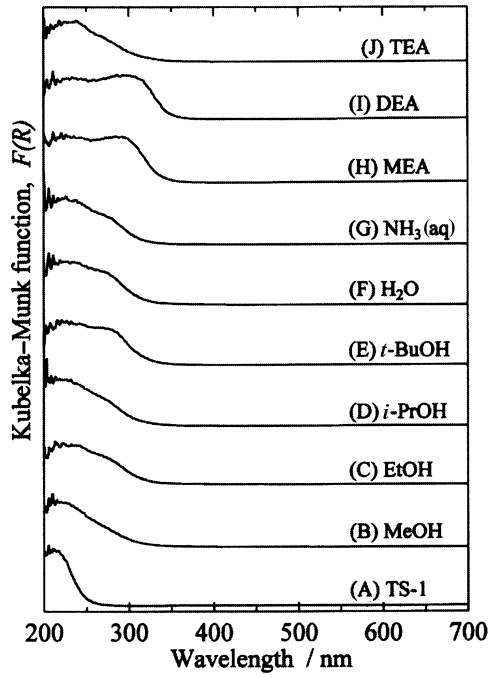

Fig. 4 DR-UV-Vis spectra of (A) TS-1 and mixtures of TS-1 with (B) MeOH, (C) EtOH, (D) Pr^{i}OH, (E) Bu^{t}OH, (F) H_2O, (G) NH_3 aq., (H) MEA, (I) DEA and (J) TEA.

groups led to more intense peaks. As mentioned above, the absorption around 300 nm may be attributed to the adsorption of organic compounds to the Ti atoms in TS-1. Therefore, it was found that alcohols with bulky alkyl group and alkanolamines were adsorbed to Ti in the framework more readily, except for TEA. Probably TEA molecules may be considered too large in molecular size to enter into the channel of the zeolite. Because the alcohols with a bulkier alkyl group among the tested ones have stronger basicity, *e.g.* $pK_a = 15$, 16 and 18 for MeOH, EtOH and Bu^{t}OH, respectively, they may adsorb more readily to Ti atom in TS-1. Consequently, a photocatalytic reaction using TS-1 was carried out *via* a degradation of MEA in diluted aqueous solution.

Fig. 2 shows UV-Vis spectra of TS-1, silicalite-1, MEA and their mixtures. Fig. 2(A) shows that the spectrum of the TS-1 specimen exhibited only absorption around 220 nm, which can be assigned to a charge transfer excitation in TiO_4 tetrahedra in the framework. On the other hand, the spectra of mixture of TS-1 and MEA showed peaks not only around 220 nm but also around 300 nm, as shown in Fig. 2(B). Fig. 2(E) and (D) show DR-UV-Vis spectra of silicalite-1, and the mixture of silicalite-1 and MEA, respectively. Silicalite-1 exhibited no particular absorption in the measured wavelength range. The mixture of silicalite-1 and MEA exhibited a peak around 210 nm. The UV-Vis spectrum of MEA shown in Fig. 2(F) exhibited absorption of UV light with wavelength shorter than 250 nm. Although the TS-1 suspension in MEA had a strong absorption around 300 nm, the spectrum of the specimen which was recovered from the suspension and annealed at 600 °C in air was consistent with that of native TS-1 as shown in Fig. 2(C), indicating that the spectral change is reversible. Therefore, it can be concluded that the peak around 300 nm is attributable not to the framework of MFI-type zeolite itself and/or its interaction with MEA but to the Ti atoms in TS-1, especially 6-fold coordinated Ti units.[33,36,45–51] The Ti sites are originally 4-fold coordinated, but the increase in the coordination number of Ti may be realized by an adsorption of organic compounds to the Ti atom, as shown in Fig. 5(a). Because original intra-framework Ti is coordinatively unsaturated and the tested organic compounds have O and/or N atoms with lone pair to be firmly

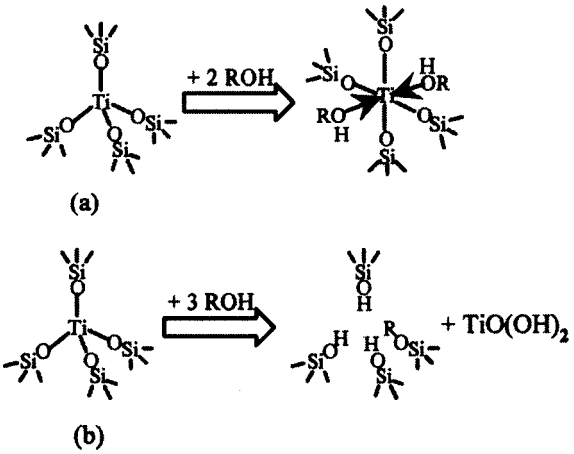

Fig. 5 Schematic diagrams of the formations of 6-fold coordinated Ti. (a) Adsorption of organic compounds to intra-framework Ti in TS-1. (b) Dropping Ti out of the framework *via* an alcoholysis reaction followed by association of the Ti atoms.

coordinatable to a metal atom. Ti–O–Ti bond formation *via* a breakage of Ti–O–Si bond in the framework, as shown in Fig. 5(b), is another possible explanation for the formation of 6-fold coordinated Ti units. However, if any, the process is irreversible, and is not consistent with the reversibility in the spectral change. It was confirmed that the formation of 6-fold coordinated Ti species is attributed to the adsorption of MEA molecules onto 4-fold coordinated intra-framework Ti atom, as shown in Fig. 5(a).

The adsorption of MEA to TS-1 was quantitatively examined using 0.12 to 0.54 mM MEA aqueous solution. After about 12 mg of the TS-1 specimen has been added into 24 ml of the MEA solutions with various concentrations, a change of MEA concentration in the solution with stirring time was measured. The same experiments were conducted also for silicalite-1 and TiO_2. For all the specimens, the MEA concentration rapidly decreased for 10 min after the addition of the specimens and the adsorption of MEA reached an equilibrium after 40 min. Relations of the equilibrated amounts of adsorbed MEA per weight of the specimens with the concentration of MEA in the solution, that is, adsorption isotherms are shown in Fig. 6. The amount of the adsorbed MEA increased in the following order: silicalite-1 $\approx$ TiO_2 $\ll$ TS-1. The data were replotted assuming Langmuir adsorption. The Langmuir adsorption is expressed in the following equation;

$$C/w = C/w_\infty + (Kw_\infty)^{-1}, \quad (1)$$

where C is a concentration of a solute in a solution, w is an amount of solute molecules adsorbed to unit weight of an adsorbent, w_∞ is an amount of adsorbed molecules when a surface of the adsorbent is completely covered *via* a mono-

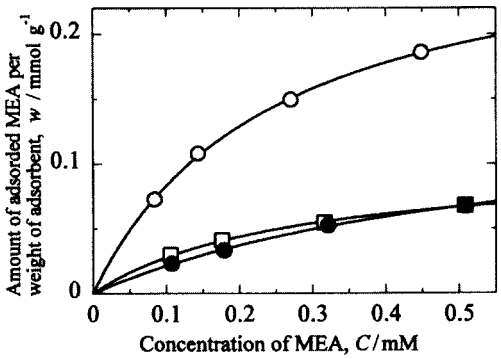

Fig. 6 Relation between amounts of MEA adsorbed to the specimens and the concentrations of MEA in the solutions, that is, adsorption isotherms for TS-1 (open circle), silicalite-1 (closed circle) and TiO_2 (open square). The amount of the specimens was 0.5 g L^{-1}.

layer adsorption, and K is an equilibrium constant of Langmuir adsorption. Fig. 7 shows the Langmuir plots for TS-1, silicalite-1 and TiO_2 specimens, all of which exhibited linear dependence. Therefore the adsorption of MEA to the specimens followed Langmuir adsorption. The intercepts and slopes in Fig. 7 show the $1/Kw_\infty$ and $1/w_\infty$, respectively. Therefore, the equilibrium constants of adsorption, K, were 4.1, 1.7, and 3.8 L $mmol^{-1}$ for TS-1, silicalite-1 and TiO_2 specimens, respectively. The values of w_∞ were 0.29, 0.14, and 0.10 mmol g^{-1} for TS-1, silicalite-1 and TiO_2 specimens, respectively. Specific surface areas were also measured *via* BET adsorption of N_2 gas, which were 421, 395, and 72 m^2 g^{-1}, for TS-1, silicalite-1, and TiO_2 specimens, respectively. The TS-1 specimen showed slightly larger surface area than silicalite-1 because Ti–O bond is longer than Si–O. The values of K and w_∞ for TS-1 were much larger than those for silicalite-1, being in good agreement with the concept shown in Fig. 4(a) that indicating that the intra-framework Ti atoms offers an additional adsorption sites of MEA. Although the value of K for TS-1 was only slightly larger than that for TiO_2, the specific surface area and w_∞ for the TS-1 specimen were much larger than those for the TiO_2 specimen because the former is a microporous material.

3.3 Photocatalytic degradation reaction of MEA using TS-1 zeolite

A photocatalytic reaction using the TS-1 specimen as a photocatalyst was examined using 0.5 mM of MEA aqueous solution. An amount of the TS-1 specimen was fixed to 0.5 g L^{-1}. UV light with the wavelength around 300 nm was irradiated. The same experiments were conducted for the suspensions containing the silicalite-1 or TiO_2 specimens and the MEA solution without TS-1 powder.

The changes of the MEA concentration with irradiation time are shown in Fig. 8. For the MEA solution without powders, the photoirradiation for 320 min led to only slight decrease in the MEA concentration from 0.5 to 0.41 mM. However, in the presence of the silicalite-1, TS-1 and TiO_2 specimens, the MEA concentration decreased from 0.46 to 0.35 mM, from 0.41 to 0.06 mM, and from 0.47 to 0.00 mM, respectively. A rate of the decrease in MEA concentration was estimated assuming that the degradation reaction of MEA is first order. When the reaction is first order, the concentration of MEA, [MEA], follows the equation of $\log([MEA]_0 : [MEA]) = kt$, where $[MEA]_0$ and k are the starting concentration of MEA and the rate constant, respectively. A sum of the concentration of MEA in the solution and the amount of MEA adsorbed to the powder specimen which was deduced from Figs. 6 and 7 was used as [MEA], assuming a negligible adsorption of the reaction products to the specimen powders. The plots of $\log([MEA]_0 : [MEA])$ *vs.* the reaction time t are shown in Fig. 9. For the TS-1 specimen, the relation of $\log([MEA]_0 : [MEA])$ with t was linear in the measured time range and the rate constant was estimated at 5.3×10^{-3} min^{-1}. On the other hand, a linear relation was not obtained for the other specimens, because the photocatalytic reaction was accompanied by some reactions such as an oxidative reaction of alcohol through aldehyde to carboxylic acid and breakage reactions of C–C or C–N bonds, as shown later. Thus, the reaction rate at an initial stage was estimated from slopes in a time range from 0 to 20 min in Fig. 9. The values of k for TiO_2, silicalite-1 and the MEA solution without powder were estimated at 6.7×10^{-2}, 2.2×10^{-3}, and 1.6×10^{-3} min^{-1}, respectively. The degradation of a small amount of MEA probably occurred even without a powder catalysis, because the wavelength range of intrinsic absorption of MEA is slightly overlapped with that of the light transmitted through the used optical filter. Although the addition of silicalite-1 caused the decomposition of slightly larger amount of MEA than in the case without powders, silicalite-1 had practically no activity as a photocatalyst. As obviously seen in Figs. 8 and 9, the photoirradiation of the MEA suspension containing the TS-1 or TiO_2 specimen led to much larger and faster decrease of the MEA concentration than for the above-mentioned other specimens, indicating that TS-1 is an effective photocatalyst similar to TiO_2. As it is natural to consider, the Ti atoms in TS-1 played an important role in the photocatalytic reaction, activities of the photocatalytic reactions per mole of Ti atoms in the specimens were compared although the activity per weight of the specimen was clearly higher for TiO_2 than for TS-1. The amounts of Ti

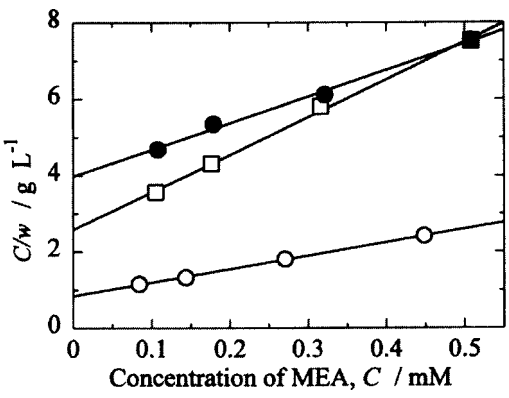

Fig. 7 Langmuir plots for adsorption of MEA to the specimens: TS-1 (open circle), silicalite-1 (closed circle) and TiO_2 (open square).

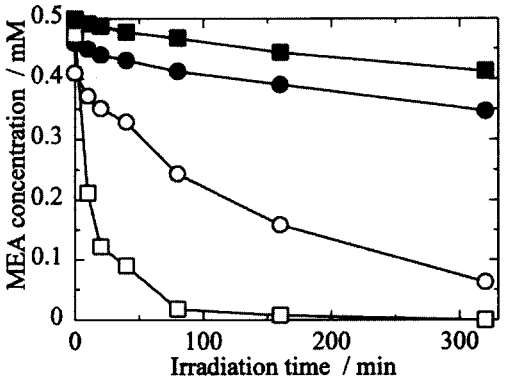

Fig. 8 Changes of MEA concentration with irradiation time of UV light in the photocatalytic reactions using TS-1 (open circle), silicalite-1 (closed circle) and TiO_2 (open square) as the photocatalyst and in the case without the powder specimen (closed square).

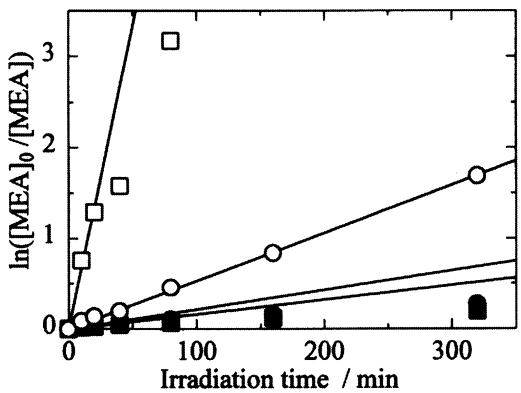

Fig. 9 Changes of MEA concentration with irradiation time, t, of UV light in the photocatalytic reactions using TS-1 (open circle), silicalite-1 (closed circle) and TiO_2 (open square) as the photocatalyst and in the case without the powder specimen (closed square). Assuming that the degradation reaction of MEA is the first order, $\ln([MEA]_0 : [MEA])$ *vs.* t was plotted. The slopes of the displayed lines show the rate constants.

atoms in the suspensions were 0.108 and 6.26 mmol L^{-1} for TS-1 and TiO_2 specimens, respectively. Thus, the decomposition rates per mole of Ti in the specimen were 49.1 and 10.6 L mol^{-1} min^{-1} for TS-1 and TiO_2 specimens, respectively. Consequently, the activity of the reaction per mole of Ti in the TS-1 specimen is about 5 times larger than that in the TiO_2 specimen. The high activity of the TS-1 specimen may be attributed to adsorption of larger amount of MEA to TS-1 as well as the microporous structure which enables all Ti atoms in TS-1 to act as reaction sites although for TiO_2 only the Ti atoms on the particle surface can do so.

The change of concentrations of the products with the irradiation time for the TS-1 specimen is shown in Fig. 10. The products were glycine (NH_2CH_2COOH), glycolic acid ($CH_2(OH)COOH$), acetic acid (CH_3COOH), formic acid (CHOOH), formamide ($CHONH_2$) and ammonia (NH_3). It was not only the oxidation of MEA to glycine but also the breakage of C–C and C–N bonds to occur *via* the photocatalytic reactions. The concentrations of glycolic acid and ammonia increased more rapidly up to 80 min than the other products. While the concentration of NH_3 increased rather steadily with the photoirradiation time, that of glycolic acid began to decrease at a later stage, that is, 80 min. Glycine began to be formed after an irradiation period of 40 min and continued to increase up to 320 min. Thus, at first the breakage of C–N bond occurs rapidly to give glycolic acid and ammonia, gradually followed by the oxidation of MEA to glycine, which is an oxidation of alcohol to carboxylic acid. In the case of TiO_2 the products were the same as in the case of the TS-1 specimen. However, the product distribution and its time dependence were somewhat different from those of TS-1. The concentrations of the products and their change up to 20 min were very similar to those for TS-1 up to 320 min. For a photoirradiation period longer than 20 min, the concentration of glycine increased up to 80 min and then decreased. The solution, which was photoirradiated for 80 min, contained MEA, ammonia, and glycine and finally that for 320 min contained only ammonia. In both cases, the concentration of C atoms in the suspensions largely decreased although that of N atoms was almost constant. This may be attributed to the removal of C component from the suspension *via* a formation of CO_2.

The influence of bubbling of O_2 and N_2 gases on photocatalytic degradation reaction of MEA was investigated in order to examine the reductive reaction. The bubbling of the gas was carried out for 60 min before the photoirradiation and also maintained during the photoirradiation. The photoirradiation was conducted using UV light with the wavelength around 300 nm through the optical filter and water.

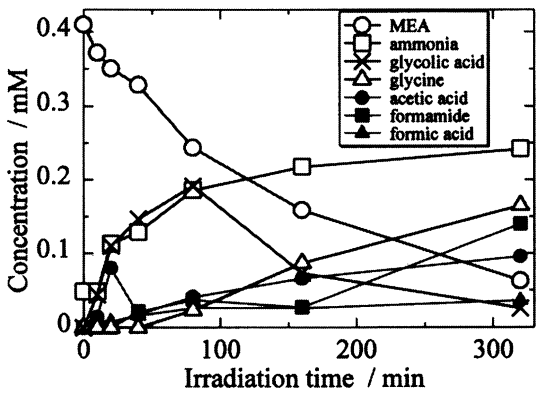

Fig. 10 Changes of concentrations of products with irradiation time of UV light in the photocatalytic reaction using TS-1 as the photocatalyst. The products are ammonia (open square), glycolic acid (cross), glycine (open triangle), acetic acid (closed circle), formamide (closed square) and formic acid (closed triangle). The change of MEA concentration is also shown (open circle).

The following are possible as the reductive reactions, that is, proton and dissolved oxygen are reduced *via* the interaction with the excited state of the Ti(IV)-ligand complex;

$$H^+ + e^- \rightarrow 1/2H_2\uparrow, \quad (2)$$

$$O_2 + e^- \rightarrow O_2^-. \quad (3)$$

If reaction (3) has a major contribution to the reduction reaction, a bubbling of O_2 gas should lead to an increase of the reaction rate of MEA while that of N_2 gas should retard it. Changes of MEA concentration with periods under photoirradiation when O_2 and N_2 gases were bubbled are shown in Fig. 11. It indicates that the bubbling of O_2 gas resulted in an increase of the reaction rate while the bubbling of N_2 gas slightly decreased it. Even under N_2 gas bubbling, that is, in the case without the presence of soluble O_2, the photocatalytic reaction did proceed. Consequently, not only reaction (3) but also other reactions, which may be related to reaction (2), may contribute as the reductive reaction, that is, the presence of soluble O_2 is not always needed for the photocatalytic reaction and the reductive reaction of H^+ to H_2 may act as the reductive reaction in the photocatalytic reaction if O_2 is not present. Since the reaction rate of the reduction of O_2 is faster than that of H^+, the presence of O_2 may facilitate the photocatalytic reaction. The effects of N_2 or O_2 gas bubbling on the product distribution were also examined. The typical results for the bubbling of N_2 are shown in Fig. 12. Glycolic acid concentration steadily increased with time and no formamide and formic acid were found in the product, dif-

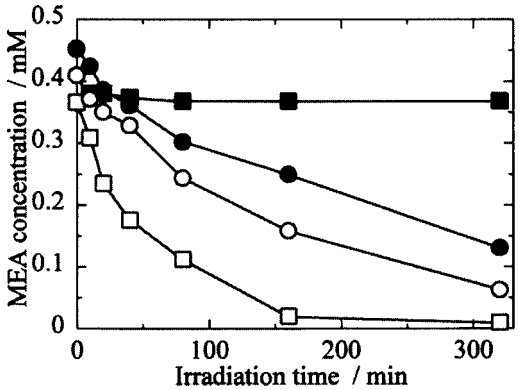

Fig. 11 Changes of concentration of MEA with irradiation time of UV light in the photocatalytic reaction using TS-1 while bubbling O_2 (open square) and N_2 (closed circle) gases. The changes in the cases of no gas-bubbling (open circle) and no irradiation while bubbling O_2 (closed square) are also shown.

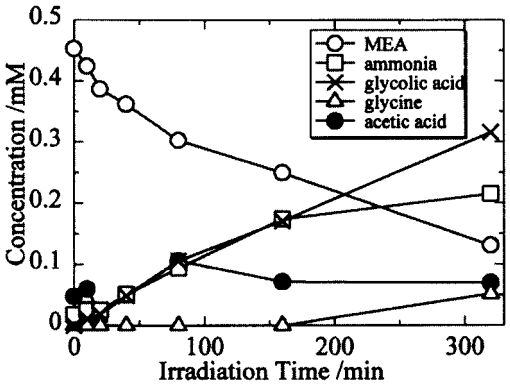

Fig. 12 Changes of concentrations of products with irradiation time of UV light in the photocatalytic reaction using TS-1 while bubbling N_2 gas. The products are ammonia (open square), glycolic acid (cross), glycine (open triangle) and acetic acid (closed circle). The change of MEA concentration is also shown (open circle).

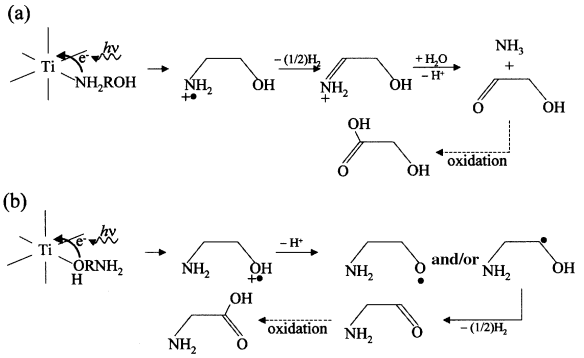

Fig. 13 Speculated reaction schemes of (a) decomposition of MEA into NH_3 and glycolic acid and (b) oxidation of MEA to glycine.

ferent from the case of no N_2-bubbling. In the presence of soluble O_2, O_2^- may be formed, which can oxidatively decompose an organic compound, which would contribute to the formations of formamide and formic acid, that is, a breakage reaction of C–C bonds. For the breakage of C–C bonds, the presence of soluble O_2 may be necessary. In the absence of soluble O_2, the photocatalytic reactions such as the oxidation of MEA to glycine and the decomposition of MEA into ammonia and glycolic acid may occur but the fission of C–C bonds may not take place.

In the photodegradation reaction of MEA, the three types of reactions occurred; (1) the breakage of C–N bond, (2) oxidation of alcohol to carboxylic acid and (3) the breakage of C–C bonds. Fig. 13 shows the reaction schemes speculated for reactions (1) and (2). When amine in MEA was datively bonded to intra-framework Ti in TS-1 to give 6-fold coordinated Ti species, charge transfer (CT) transition in the dative bond of Ti–N may lead to the breakage of the C–N bond in MEA, resulting in the formation of NH_3 and glycolic acid. This reaction began to occur immediately after the photoirradiation. On the other hand, when alcohol in MEA was datively bonded to intra-framework Ti, CT transition in the dative bond of Ti–O may lead to the oxidation of alcohol in MEA to carboxylic acid, resulting in the formation of glycine. This reaction occurred after an induction period. As mentioned above, O_2^-, which was formed *via* the reduction of soluble O_2, may be attributed to the breakage of the C–C bond although details of the reaction were not obvious.

4 Conclusions

A photocatalytic degradation reaction of MEA was examined using TS-1 zeolite as a photocatalyst. The following conclusions were drawn:

(1) A mixing of TS-1 with MEA led to a change of coordinative situations around Ti atom, that is, a coordination number of Ti was changed from 4 to 6 *via* an adsorption of MEA to Ti. The change in the coordination number of Ti shifted the absorption by a charge transfer excitation from 220 to 300 nm.

(2) Larger amount of MEA was adsorbed to TS-1 than to silicalite-1 and TiO_2. This may be attributed to the adsorption of MEA to the intraframework Ti.

(3) A photoirradiation of UV light with the wavelength of around 300 nm to a mixture of MEA aqueous solution and TS-1 caused a photocatalytic degradation of MEA. Although an activity of the reaction per weight of the specimen was lower for TS-1 than for TiO_2, that per mole of Ti atom in TS-1 was higher than that in TiO_2.

(4) No differences in products and changes of their concentrations were observed in the photocatalytic reactions. At first, a breakage of the C–N bond in MEA occurred rapidly resulting in the formation of NH_3 and glycolic acid. At a second stage, an oxidation of MEA to glycine occurred gradually.

(5) Both reductions of dissolved oxygen and H^+ might contribute to the photocatalytic reaction. A decomposition by O_2^- formed *via* the reduction of dissolved oxygen may contribute to a breakage of the C–C bond.

As the photocatalytic degradation reaction of MEA occurred *via* the photoexcitation of the MEA-adsorbed Ti species, a realization of the photocatalytic reaction with a molecular selectivity is expected. The investigations of the photocatalytic reaction with a molecular selectivity are in progress and their results will be presented elsewhere.

References

1 G. A. Ozin, A. Kuperman and A. Stein, *Angew. Chem. Int. Ed. Engl.*, 1989, **28**, 359.
2 J. M. Thomas, *Angew. Chem. Int. Ed. Engl.*, 1988, **27**, 1673.
3 G. D. Stucky and J. E. MacDougall, *Science* (Washington, D.C.), 1990, **247**, 669.
4 M. E. Davis, *Acct. Chem. Res.*, 1993, **26**, 111.
5 J. M. Newsam, *Science* (Washington, D.C.), 1986, **231**, 1093.
6 M. Taramasso, G. Perego and B. Natori, *U. S. Patent*, 4410501, 1983.
7 A. Thangaraj, R. Kumar, S. P. Mirajjkar and P. Ratnasamy, *J. Catal.*, 1991, **130**, 1.
8 J. S. Reddy and R. Kumar, *J. Catal.*, 1991, **130**, 440.
9 T. Tatsumi, K. Yanagisawa, K. Asano, M. Nakamura and H. Tominaga, *Stud. Surf. Sci. Catal.*, 1994, **83**, 417.
10 A. Tuel and Y. B. Taarit, *Appl. Catal.*, 1993, **102**, 69.
11 T. Tatsumi, K. Yuasa and H. Tominaga, *J. Chem. Soc., Chem. Commun.*, 1992, 1446.
12 A. Tuel, *Zeolites*, 1995, **15**, 236.
13 P. R. H. P. Rao, A. V. Ramaswamy and P. Ratnasamy, *J. Catal.*, 1992, **137**, 225.
14 A. V. Ramaswamy, S. Sivasanker and P. Ratnasamy, *Microporous Mater.*, 1994, **2**, 451.
15 A. Tuel and Y. B. Taarit, *Zeolites*, 1994, **14**, 18.
16 T. Sen, M. Chatterjee and S. Sivasanker, *J. Chem. Soc., Chem. Commun.*, 1995, 207.
17 G. I. Panov, G. A. Sheveleva, A. S. Kharitonov, V. N. Romannikov and L. A. Vostrikova, *Appl. Catal.*, 1992, **82**, 31.
18 S. Bordiga, R. Buzzoni, F. Geobaldo, C. Lamberti, E. Giamello, A. Zecchina, G. Leofanti, G. Petrini, G. Tozzola and G. Vlaic, *J. Catal.*, 1996, **158**, 486.
19 Y. S. Ko and W. S. Ahn, *Microporous Mater.*, 1997, **9**, 131.
20 A. Tavolaro, *J. Therm. Anal.*, 1996, **47**, 171.
21 A. P. Singh and T. Selvam, *J. Mol. Catal. A: Chem.*, 1996, **113**, 489.
22 P. S. Raghavan, V. Ramaswamy, T. T. Upadhya, A. Sudalai, A. V. Ramaswamy and S. Sivasanker, *J. Mol. Catal. A: Chem.*, 1997, **122**, 75.
23 B. Rakshe, V. Ramaswamy, S. G. Hegde, R. Vetrivel and A. V. Ramaswamy, *Catal. Lett.*, 1997, **45**, 41.
24 Y. Ichihashi, H. Yamashita and M. Anpo, *Abstrct 11th Int. Zeolite, Conf., Seoul*, 1996, p. 129.
25 M. Anpo and K. Chiba, *J. Mol. Catal.*, 1992, **74**, 207.
26 M. Anpo, H. Yamashita, Y. Ichihashi and S. Ehara, *J. Electroanal. Chem.*, 1995, **396**, 21.
27 H. Yamashita, Y. Ichihashi, M. Harada, G. Stewart and M. A. Fox., *J. Catal.*, 1996, **158**, 97.
28 K. Kosuge and P. S. Singh, *Chem. Lett.*, 1999, 9.
29 S. G. Zhang, Y. Fujii, H. Yamashita, K. Koyano, T. Tatsumi and M. Anpo, *Chem. Lett.*, 1997, 659.
30 Y. Ichihashi, H. Yamashita and M. Anpo, *Stud. Surf. Sci. Catal.*, 1997, **105**, 1609.
31 M. Anpo, H. Yamashita, K. Ichihashi, K. Ikeue, Y. Fujii, Y. Ichihashi, S. G. Zhang, D. R. Park, S. Ehara, S.-E. Park, J.-S. Chang and J. W. Yoo, *Stud. Surf. Sci. Catal.*, 1998, **114**, 177.
32 S. G. Zhang, Y. Ichihashi, H. Yamashita, T. Tatsumi and M. Anpo, *Chem. Lett.*, 1996, 895.
33 L. L. Noc, D. T. On, S. Solomykina, B. Echchahed, F. Béland, C. C. dit Moulin and L. Bonneviot, *Stud. Surf. Sci. Catal.*, 1996, **101**, 611.
34 A. Zecchina, S. Bordiga, C. Lamberti, G. Ricchiardi, D. Scarano, G. Petrini, G. Leofanti and M. Mantegazza, *Catal. Today*, 1996, **32**, 97.
35 S. Bordiga, S. Coluccia, C. Lamberti, L. Marchese, A. Zecchina, F. Boschrini, F. Buffa, F. Genoni, G. Leofanti, G. Petrini and G. Vlaic, *J. Phys. Chem.*, 1994, **98**, 4125.
36 L. Marchese, T. Maschmeyer, E. Gianotti, S. Coluccia and J. M. Thomas, *J. Phys. Chem. B*, 1997, **101**, 8836.

37 S. Bordiga, F. Geobaldo, C. Lamberti, A. Zecchina, F. Boscherini, F. Genoni, G. Leofanti, G. Perrini, M. Padonvan, S. Geremia and G. Vlaic, *Nucl. Instrum. Methods Phys. Res., Sect. B*, 1995, **97**, 23.
38 S. Bordiga, F. Boscherini, S. Coluccia, F. Genoni, C. Lamberti, G. Leofanti, L. Marchese, G. Petrini, G. Vlaic and A. Zecchina, *Catal. Lett.*, 1994, **26**, 195.
39 C. Lamberti, S. Bordiga, A. Zecchina, G. Vlaic, G. Tozzola, G. Petrini and A. Carati, *J. Phys. IV*, 1997, **7**, C2-851.
40 T. Maschmeyer, F. Rey, G. Sankar and J. M. Thomas, *Nature* (*London*), 1995, **378**, 159.
41 T. Blasco, M. A. Camblor, A. Corma and J. Pérez-Pariente, *J. Am. Chem. Soc.*, 1993, **115**, 11806.
42 F. Izumi, in *The Rietveld Method*, ed. R. A. Young, Oxford University Press, Oxford, 1993, ch. 13.
43 G. Kortüm, in *Reflections Spectroskopie*, Springer-Verlag, Berlin, 1969.
44 H. van Koningsveld, H. van Bekkum and J. C. Jansen, *Acta Crystallogr.*, 1987, **B43**, 127.
45 G. Grubert, M. Wark, N. I. Jaeger, G. Sculz-Ekloff and O. P. Tkachenko, *J. Phys. Chem. B*, 1998, **102**, 1665.
46 A. Zecchina, G. Spoto, S. Bordiga, A. Ferrero, G. Petrini, M. Pandovan and G. Leofanti, *Stud. Surf. Sci. Catal.*, 1991, **69**, 251.
47 Y. L. Kim, R. L. Riley, M. J. Huq, S. Salim, A. E. Le and T. E. Mallouk, *Mater. Res. Soc. Symp. Proc.*, 1991, **233**, 145.
48 S. Klein, B. M. Weckhuysen, J. A. Marteno, W. F. Maier and P. A. Jacobs, *J. Catal.*, 1996, **163**, 489.
49 S. V. Lysak and B. Y. Sukhaoevskii, *Dokl. Acad. Nauk SSSR*, 1969, **188**, 1299.
50 M. R. Boccuti, K. M. Rao, A. Zecchina, G. Leofanti and G. Petrini, *Stud. Surf. Sci. Catal.*, 1989, **48**, 133.
51 G. Petrini, A. Cesana, G. deAlberti, F. Genoni, G. Leofanti, M. Padovan, G. Paparatto and P. Rofia, *Stud. Surf. Sci. Catal.*, 1991, **68**, 761.
52 A. Zecchina, G. Spoto, S. Bordiga, M. Padovan, G. Leofanti and G. Petrini, *Stud. Surf. Sci. Catal.*, 1991, **65**, 671.
53 D. Scarano, A. Zecchina, S. Bordiga, F. Geobaldo, G. Spoto, G. Patrini, G. Leofanti, M. Pandovan and G. Tozzola, *J. Chem. Soc., Faraday Trans.*, 1993, **89**, 4123.
54 G. Bellussi, A. Carati, M. G. Clerici, G. Maddinelli and R. Minili, *J. Catal.*, 1992, **133**, 220.
55 A. Tuel, *Stud. Surf. Sci. Catal.*, 1997, **105**, 261.

Paper 9/06585G